

# Stochastic Subnetwork Annealing: A Regularization Technique for Fine Tuning Pruned Subnetworks

Tim Whitaker

*Department of Computer Science  
Colorado State University  
Fort Collins, CO, USA  
timothy.whitaker@colostate.edu*

Darrell Whitley

*Department of Computer Science  
Colorado State University  
Fort Collins, CO, USA  
whitley@cs.colostate.edu*

**Abstract**—Pruning methods have recently grown in popularity as an effective way to reduce the size and computational complexity of deep neural networks. Large numbers of parameters can be removed from trained models with little discernible loss in accuracy after a small number of continued training epochs. However, pruning too many parameters at once often causes an initial steep drop in accuracy which can undermine convergence quality. Iterative pruning approaches mitigate this by gradually removing a small number of parameters over multiple epochs. However, this can still lead to subnetworks that overfit local regions of the loss landscape. We introduce a novel and effective approach to tuning subnetworks through a regularization technique we call Stochastic Subnetwork Annealing. Instead of removing parameters in a discrete manner, we instead represent subnetworks with stochastic masks where each parameter has a probabilistic chance of being included or excluded on any given forward pass. We anneal these probabilities over time such that subnetwork structure slowly evolves as mask values become more deterministic, allowing for a smoother and more robust optimization of subnetworks at high levels of sparsity.

## I. INTRODUCTION

Deep neural networks have seen a steady increase in size as large amounts of compute and high quality data have become more accessible. Models with billions of parameters are becoming commonplace and demonstrating incredible performance across a wide range of difficult machine learning tasks. However, these models also bring important challenges related to computational needs, storage cost, and training efficiency. The resource-intensive nature of these large networks have spurred a growing interest in techniques that can reduce the size and computational complexity associated with training and deploying these models.

One of the most popular methods used to compress large networks is weight pruning. It's long been known that you can remove a significant number of parameters from these trained models, and after a small number of epochs of continued training, they can maintain or even exceed the performance of the full size network [1], [5]. While saliency metrics are often used to prune the most unnecessary weights, even random sampling has been shown to produce accurate models at moderate levels of sparsity [27].

Several researchers have investigated ways to tune these subnetworks more efficiently and with better accuracy. One of the most effective techniques used in state of the art pruning methods involves iterative pruning/tuning cycles [1]. The key

insight being that pruning too many parameters at once can lead to drastic performance collapse as subnetworks get stuck in lower performing regions of the optimization landscape. Pruning a small number of parameters over several epochs allows the model to better adapt to the changing network structure. However, these iterative methods can still result in subnetworks that are prone to overfitting local optimization regions.

We introduce a novel regularization approach for fine tuning these subnetworks by leveraging stochasticity for the network structure. Rather than using fixed subnetworks and discrete pruning operations, we instead represent subnetworks with probability matrices that determine how likely it is that a parameter is retained on any given forward pass. The probability matrices are then adjusted during the tuning phase through the use of dynamic annealing schedules which allows for a subnetwork to be slowly revealed over several epochs. The probabilistic inclusion of extra parameters early in the tuning process allows for gradient information to bleed through into the target subnetwork, encouraging robust adaptation and avoiding the drastic performance collapse observed with one-shot pruning methods.

We conduct a large scale ablation study with ResNets and Vision Transformers to explore the efficacy and dynamics of several hyperparameters and their effects on convergence, including: degree of stochasticity, number of annealing epochs, amount of sparsity, constant/phasic learning rate schedules, and random/saliency based parameter selection strategies. Our experiments demonstrate significant improvements over both one-shot and iterative pruning methods across several tuning configurations with especially large improvements in highly sparse convolutional subnetworks (95-98%).

We additionally explore how Stochastic Subnetwork Annealing can be leveraged in a benchmark low-cost ensemble learning method that generates diverse child networks through random pruning of a trained parent network. Implementing our technique to tune the child networks results in better ensemble generalization on benchmark image classification tasks, improving on the training compute/accuracy Pareto Frontier for efficient ensemble methods.

## II. BACKGROUND

Subnetworks are represented with binary bit mask matrices with the same dimensions of the weight matrices for each layer in the parent network. Consider a weight matrix  $W \in \mathbb{R}^{m \times n}$  representing the weights of a particular layer in a neural network. We introduce a matrix  $M \in \{0, 1\}^{m \times n}$  with the same dimensions as  $W$ . The elements of  $M$  are binary values, where  $M_{ij} = 1$  if the corresponding weight  $W_{ij}$  is retained, and  $M_{ij} = 0$  if the weight is masked. The mask is generated with an arbitrary discrete stochastic process  $\phi$ . The subnetwork weights  $\hat{W}$  can then be computed as the element-wise (Hadamard) product of  $W$  and  $M$ .

$$M \sim \phi^{m \times n} \quad (1)$$

$$\hat{W} = W \circ M \quad (2)$$

The topology of the subnetwork can be further described by the granularity in which parameters are masked. This granularity refers to the unstructured or structured distribution of masked weights, where unstructured methods refer to weight-level or connection-level masking and structured methods refer to neuron-level, channel-level, or layer-level masking. Removing entire rows, columns, or blocks from a layer's weight matrix can be effective at reducing computational complexity as the reduced size of the weight matrix can be leveraged for hardware optimizations. This is more difficult to achieve with the sparse matrices resulting from unstructured masking. However, unstructured masking tends to result in networks with better generalization as the number of masked parameters increases [1]. We choose to use unstructured masking for our experiments with Stochastic Annealing due to the higher sparsity potential, however our work is fully compatible with structured methods.

It's important to also consider the distribution of masked weights throughout non-homogenous networks. It's common for layer configurations in deep neural networks to vary significantly in size and shape. Severe pruning of small layers may result in bottlenecks that restrict gradient flow. The distribution of masked weights can be controlled with global and local masking methods where global methods are applied uniformly across the entire network while local methods are applied independently within each layer or sub-region. Global methods tend to result in higher compression rates as more parameters from the larger layers are removed whereas local methods offer more fine-grained control and reduced variance [1].

Iterative pruning has been shown to be highly effective at improving accuracy of subnetworks compared to one-shot pruning [5], [6], [10], [23]. Instead of pruning all of the weights at once, instead an iterative cycle is implemented where a small number of weights are pruned, the network is tuned, and this repeats until a target sparsity level is reached. Iterative pruning results in a less destructive effect on network performance which can allow for greater levels of sparsity at improved accuracy.

### A. Optimizing Pruned Subnetworks

Continued training of the subnetwork is crucial in order to recover the lost accuracy from pruning. Only a small number of epochs are generally needed as subnetworks inherited from trained networks tend to converge quickly. The standard practice for fine-tuning subnetworks involves training with a small constant learning rate consistent with the final phase of the parent network's training procedure [10], [23], [28].

The Lottery Ticket Hypothesis introduced the concept of weight rewinding, where both the network weights and the learning rate is rewound to a previous state  $t$  epochs ago. Training continues from this previous state but with the new subnetwork structure fixed [5]. Subsequent research has shown that rewinding both the weights and the learning rate is less effective than rewinding only the learning rate itself [35].

The efficacy of learning rate rewinding has been tangentially observed in many optimization papers where a decaying learning rate schedule improves the training efficiency and convergence quality in deep networks [44]. The one-cycle policy is one such schedule, which consists of a warm-up phase that anneals from a small learning rate to a large learning rate, followed by a cosine annealed cool-down to a very small value. This schedule can lead to a phenomenon called super-convergence, where network training is greatly accelerated on some datasets [36]. This kind of phasic learning rate schedule is effective when the number of tuning epochs is relatively small, as seen in several efficient ensemble methods, as large learning rates help to encourage more movement in parameter space before using small learning rates to converge to local optima [7], [15], [36], [42].

### B. Probabilistic Subnetworks

Several researchers have explored the connection between stochasticity and sparse network structure. The most prominent example being Dropout, which randomly disables neurons on every forward pass during training according to a layer-wise constant probability value [37]. Variational and Adaptive Dropout methods introduced a probabilistic approach to determining the importance of neurons by learning optimal dropout rates during training [17], [21], [32]. Sparsity inducing regularization techniques have been used to prune networks during training by incorporating additional loss terms and learning objectives [23], [24], [40]. Probabilistic gating techniques have also been used to route signals through sparse network paths and is effective in multi-task or continual learning environments [4], [14]. While these methods leverage stochasticity to find sparse network structures, they often require special training procedures, network architectures, or are limited in that they learn only a single subnetwork throughout the entirety of training. Stochastic Subnetwork Annealing has a completely distinct methodology and purpose by instead focusing on improving the optimization of any randomly sampled subnetwork from any fully trained model in a small number of epochs.

### III. STOCHASTIC SUBNETWORK ANNEALING

In pruning literature, sparse network structures are generally static and represented with binary bit masks. We propose a model of representing neural subnetworks with probabilistic masks, where each parameter is assigned a score that determines how likely it is that the parameter will be retained on any given forward pass. This introduces stochasticity into the subnetwork sampling process, which can act as a form of implicit regularization analogous to a reverse dropout, where parameters that would have been pruned have a chance to activate. This technique encourages exploration of a larger space of subnetworks during the fine-tuning phase, preventing it from becoming overly reliant on a single fixed topological configuration, resulting in more robust and generalized subnetworks.

Consider a weight matrix  $W \in \mathbb{R}^{m \times n}$  representing the weights of a particular layer in a neural network. We introduce a probability matrix  $P \in \mathbb{R}^{m \times n}$  containing scores that represent the probability that a parameter  $W_{ij}$  will be masked on any given forward pass. The subnetwork mask  $M \in \{0, 1\}^{m \times n}$  is determined with a Bernoulli realization of the probability matrix  $P$ .

We then anneal these probability values over some number of epochs such that subnetworks are slowly "revealed" throughout fine-tuning. This is done by introducing an annealing schedule, where the probability values for each parameter slowly move towards 0 or 1 depending on the target subnetwork sparsity. At the beginning of the training process, a high level of stochasticity is desirable as it encourages exploration of the weight space which may help to prevent overfitting and search for more effective subnetwork configurations. As training progresses, the stochasticity should gradually decrease via some decay function (linear, cosine, exponential, etc.) to allow for stable convergence over several epochs.

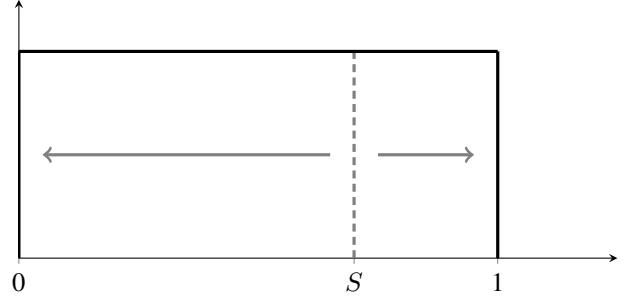
$$y_{lin}(t) = \tau_{max} - (\tau_{max} - \tau_{min}) \left( \frac{t}{T_{max}} \right) \quad (3)$$

$$y_{cos}(t) = \tau_{min} + \frac{1}{2}(\tau_{max} - \tau_{min}) \left( 1 + \cos \left( \frac{t}{T_{max}} \right) \right) \quad (4)$$

where  $(\tau_{max}, \tau_{min})$  are the initial and final leaning rates,  $t$  is the current time step, and  $T_{max}$  is the total number of annealing steps.

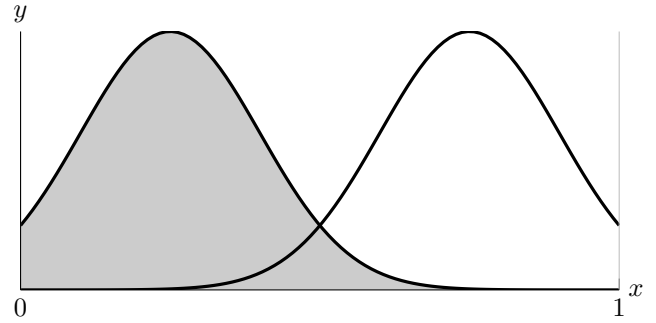
#### A. Random Annealing

The probability matrix can be generated in arbitrary ways. For example, a uniform distribution  $P \sim U([0, 1])^{m \times n}$  can be used to randomly assign probabilities to each parameter. All parameters with a value less than the sparsity target will then anneal towards 0 while parameters with a probability value greater than the sparsity target will anneal towards 1.



With this implementation, the mean activation of parameters at the beginning of tuning will be 50% regardless of the target subnetwork sparsity. Other distributions can offer more fine grained control over network structure. For example, assume that a binary matrix  $X \in \{0, 1\}^{m \times n}$  is randomly generated and used to index into a probability matrix  $P \in \mathbb{R}^{m \times n}$ . Using this index matrix  $X$ , we can sample from Gaussian distributions with different means and variances.

$$P = \begin{cases} P_{ij} \sim \mathcal{N}(\mu_1, \sigma_1^2), & \text{if } X_{ij} = 0 \\ P_{ij} \sim \mathcal{N}(\mu_2, \sigma_2^2), & \text{if } X_{ij} = 1 \end{cases}$$



This approach to constructing multi-modal distributions can allow for interesting formulations of stochastic subnetworks. Future work may find natural applications to multi-task learning, where certain groups of parameters can be strongly correlated with each other while allowing for overlap with other task specific subnetworks. This stochastic overlap may encourage shared portions of the network to learn generalized features, avoiding the problem in typical network-splitting approaches where task specific subnetworks become increasingly narrow with degraded performance.

#### B. Temperature Annealing

Temperature scaling may be applied to binary matrices in order to allow for an even application of stochasticity, reducing some variance relative to random annealing. Assume that some binary matrix  $X \in \{0, 1\}^{m \times n}$  is generated to represent a target subnetwork. A temperature scaling constant  $\tau$  is introduced such that the values in  $X$  with a 1 are decayed by  $\tau$  and the values with 0 are increased by  $\tau$ . The mask is then determined on every forward pass with an altered probability according to  $\tau$ . Altering the initial value of  $\tau$  allows for a much more controlled approach to noise injection during the early phases

of tuning, which can be highly desirable when the number of total tuning epochs is limited.

A variation of temperature scaling, where tau is only applied to parameters that are not a part of the target subnetwork, will be shown to be a highly effective form of regularization analogous to a reverse dropout. That is, the subnetwork is always active, but parameters that would have been pruned away now have a chance to pop back in during tuning. This formulation is less destructive than full temperature scaling as the target subnetwork will be optimized on every training step. Allowing other parameters to become active allows for gradient information to contribute to optimization of the target subnetwork which can help to encourage avoidance of local minima.

$$P = \begin{bmatrix} 1 & 1 & 0 + \tau & 1 \\ 0 + \tau & 1 & 0 + \tau & 0 + \tau \\ 1 & 0 + \tau & 0 + \tau & 1 \\ 0 + \tau & 0 + \tau & 1 & 1 \end{bmatrix}$$

#### IV. EXPERIMENTS

##### A. Ablations

We begin with an exploration of several stochastic subnetwork annealing configurations with the goal of investigating how different hyperparameters impact the efficiency and quality of subnetwork convergence, compared to established one-shot and iterative pruning techniques.

We use the benchmark CIFAR-10/CIFAR-100 datasets to conduct our explorations [18]. CIFAR consists of 60,000 small natural colored images that are 32x32 pixels in size. Each dataset is split into a training set containing 50,000 images and a test set containing 10,000 images. CIFAR-10 samples images from 10 different classes, or target labels, while CIFAR-100 samples from 100 different classes. Thus, CIFAR-10 contains 5,000 images for each class while CIFAR-100 is comparatively more difficult containing only 500 images for each class.

All ablations use the same ResNet-18 trained for 100 epochs using a standardized optimization configuration [13]. We use PyTorch’s Stochastic Gradient Descent optimizer with an initial learning rate of 0.1 and Nesterov momentum of 0.9. After 50 epochs, the learning rate is decayed to 0.01 and again to 0.001 for the final 10 epochs. We use standard data augmentations including random crop, random horizontal flip, and mean standard normalization.

Pruning is done in a layerwise unstructured fashion, after which each subnetwork is tuned for an additional 20 epochs. We experiment with both a constant learning rate of 0.01 and a one-cycle policy with a max learning rate of 0.1. We explore the results for each configuration with different levels of final subnetwork sparsity  $\rho \in [0.5, 0.7, 0.9, 0.95, 0.98]$ . We additionally include results for subnetworks created through L1 unstructured pruning. In this case, parameters with the smallest magnitudes at each layer are pruned.

The one-shot baseline prunes the parent network to the target sparsity before we start tuning. Iterative pruning calculates

the number of parameters to remove at the beginning of each epoch over some number of pruning epochs  $\varphi \in [5, 10, 15, 20]$  such that the final target sparsity is hit. Random Annealing uses a probability matrix that is generated according to a random uniform distribution, where each parameter is assigned a value between 0 and 1. Parameters with a value less than the target sparsity value are linearly annealed to 0 and values greater than the target sparsity are linearly annealed to 1, over some number of annealing epochs  $\varphi \in [5, 10, 15, 20]$ . Temperature Annealing uses a randomly generated binary bitmask according to the target sparsity. All parameters with a value of 0 are modified to an initial temperature value of  $\tau \in [0.2, 0.4, 0.6, 0.8, 1.0]$ . Those values are then cosine annealed to 0 over some number of annealing epochs  $\varphi \in [5, 10, 15, 20]$ .

Table 1 includes the mean accuracies for the best configurations of each method on CIFAR-100. We see consistent improvement with both of our stochastic annealing methods over the baseline one-shot and iterative pruning techniques across all sparsities and with both a constant learning rate and a one-cycle policy. As networks become more sparse, the benefits from our annealing approaches become more significant, with a 6% and 4% improvement at 98% sparsity over the one-shot baseline with a constant and one-cycle rate schedule respectively. We also observed improved performance with magnitude pruning, however the differences were smaller at 2% and 1% improvement respectively.

Figure 1 includes an exploration of the initial temperature, the number of annealing epochs and the test trajectories for the best models tuned with a constant learning rate schedule. The hyperparameter with the most significant impact on all pruning methodologies was the number of epochs that were pruned or annealed over. We saw best results for all subnetwork sparsities with  $e = 5$  or  $e = 10$  annealing epochs. It’s important for the final subnetwork topology to be established for a sufficient number of epochs to allow for optimal convergence behavior. This pattern holds for both constant and one-cycle learning rate schedules. The initial temperature has a smaller impact on performance than the number of annealing epochs. A small value of  $\tau$  means that the target subnetwork is always active and other parameters have a small chance to turn on, while a high value of  $\tau$  gives other parameters a high chance to turn on. We saw best results when  $\tau$  was in the 0.4 to 0.6 range. This corresponds to a higher state of entropy regarding network structure which results in a stronger regularization effect for those initial training examples.

Figure 2 includes an exploration of random annealing vs temperature annealing, iterative pruning vs temperature annealing, and the test trajectories for the best models with a one-cycle learning rate schedule. Despite the additional variance associated with random annealing, we found that the performance was very good and nearly approached that of temperature annealing. Temperature annealing consistently outperformed iterative pruning. The graph displays results for annealing epochs  $e \in [5, 10]$  and a target subnetwork sparsity of 0.9. While the early accuracy of temperature annealing appears worse, it quickly surpasses iterative pruning as the

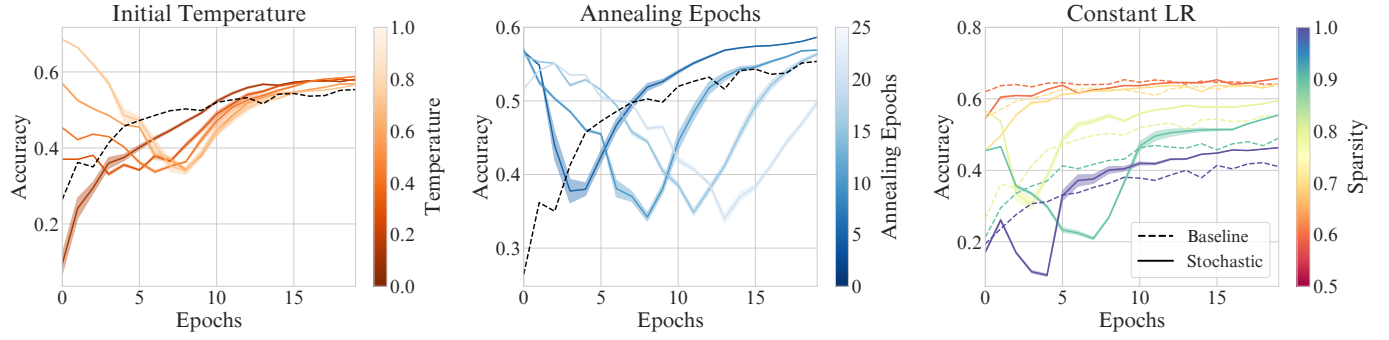


Fig. 1. Ablations exploring how the initial temperature and the number of annealing epochs affect convergence behavior. The rightmost graph displays the best performing annealing configuration for each sparsity and plots it against the one-shot pruning baseline. Stochastic annealing outperformed the other methods for each sparsity, with more drastic improvements appearing in extremely sparse networks.

Table I. Comparison between various baseline approaches when used with random/magnitude pruning on CIFAR-100. We report the best accuracy for each method at various levels of target sparsity when tuned with both a constant learning rate and a one-cycle learning rate schedule. The parent network has a baseline accuracy of 71.5%. Our annealing strategies consistently outperform established one-shot and iterative pruning methods.

Resnet-18/CIFAR-100	Method	50%	70%	90%	95%	98%
Random/Constant	One-Shot Baseline	$64.0 \pm 0.07$	$63.4 \pm 0.13$	$54.9 \pm 0.12$	$48.4 \pm 0.24$	$41.1 \pm 0.47$
	Iterative Pruning	$65.1 \pm 0.10$	$63.4 \pm 0.05$	$57.8 \pm 0.06$	$49.8 \pm 0.22$	$42.8 \pm 0.26$
	Random Annealing	$65.3 \pm 0.17$	$63.6 \pm 0.15$	$58.9 \pm 0.17$	$54.5 \pm 0.16$	$45.7 \pm 0.22$
	Temperature Annealing	$65.6 \pm 0.09$	$64.3 \pm 0.12$	$59.5 \pm 0.02$	$55.4 \pm 0.19$	$46.5 \pm 0.15$
Random/One-Cycle	One-Shot Baseline	$70.1 \pm 0.07$	$68.9 \pm 0.19$	$61.8 \pm 0.07$	$56.8 \pm 0.21$	$49.3 \pm 0.27$
	Iterative Pruning	$70.1 \pm 0.03$	$69.2 \pm 0.11$	$63.9 \pm 0.05$	$57.4 \pm 0.12$	$49.8 \pm 0.51$
	Random Annealing	$70.2 \pm 0.09$	$69.2 \pm 0.12$	$64.5 \pm 0.07$	$59.7 \pm 0.16$	$52.7 \pm 0.30$
	Temperature Annealing	$70.6 \pm 0.06$	$69.6 \pm 0.09$	$64.9 \pm 0.08$	$60.2 \pm 0.08$	$53.3 \pm 0.29$
Magnitude/Constant	One-Shot Baseline	$67.1 \pm 0.16$	$67.3 \pm 0.37$	$65.7 \pm 0.24$	$63.3 \pm 0.14$	$54.4 \pm 0.24$
	Iterative Pruning	$68.2 \pm 0.09$	$67.9 \pm 0.04$	$65.9 \pm 0.07$	$63.3 \pm 0.02$	$56.2 \pm 0.11$
	Temperature Annealing	$68.5 \pm 0.03$	$68.3 \pm 0.03$	$66.3 \pm 0.02$	$63.4 \pm 0.11$	$56.6 \pm 0.19$
Magnitude/One-Cycle	One-Shot Baseline	$70.9 \pm 0.12$	$70.1 \pm 0.26$	$69.7 \pm 0.06$	$67.5 \pm 0.16$	$60.2 \pm 0.10$
	Iterative Pruning	$71.1 \pm 0.04$	$71.1 \pm 0.06$	$69.9 \pm 0.16$	$67.6 \pm 0.08$	$60.8 \pm 0.19$
	Temperature Annealing	$71.5 \pm 0.06$	$71.4 \pm 0.02$	$70.3 \pm 0.10$	$67.8 \pm 0.02$	$61.5 \pm 0.02$

annealing phase ends. The One-Cycle schedule does reduce the accuracy gap between our method and the baselines due to the much improved generalization compared to the constant learning rate models. However, temperature annealing still consistently outperformed the baseline across all sparsities.

## B. Vision Transformers

We also include a comparison of temperature annealing and one-shot pruning with modern vision transformer networks on the Tiny Imagenet benchmark [3], [20]. Borrowing from their natural language counterparts, Vision Transformers make use of attention mechanisms and multilayer perceptrons. These models are quickly growing in popularity as they continue to produce state-of-the-art results on large scale and difficult image classification tasks [46]. For our ablation experiments, we use an open source implementation of the Vision Transformer with hyperparameters selected to be appropriate for small scale datasets [34]. These include twelve transformer encoder layers and twelve attention heads where each encoder contains a self attention block with a hidden size of 384 followed by a two

layer MLP with an expansion factor of 4 for a hidden size of 1536.

The parent models are trained for 200 epochs using Adam with a learning rate of 1e-4, weight decay of 5e-5, and a batch size of 128. We incorporate a warmup phase for 5 epochs where the learning rate is linearly increased from 0 to 1e-4 which is known to reduce divergent variance between runs [29]. Standard data augmentation schemes are used including random crop, random horizontal flip, and autoaugment [2].

We then implement the one-shot pruning and temperature annealing approaches for target subnetworks of various levels of sparsity  $s \in [0.5, 0.6, 0.7, 0.8, 0.9]$ . Subnetworks are trained for 20 additional epochs with both the stochastic gradient descent and adam optimizers [16]. We additionally explore the efficacy of the one-cycle learning rate schedule with both of these optimizers. With SGD, the constant configuration uses a learning rate of 1e-2 and the one-cycle learning rate uses a maximum value of 1e-1, both with a momentum value of 0.9. With Adam, the constant configuration uses a learning rate of 1e-3 and the one-cycle learning rate uses a maximum value of 1e-2.

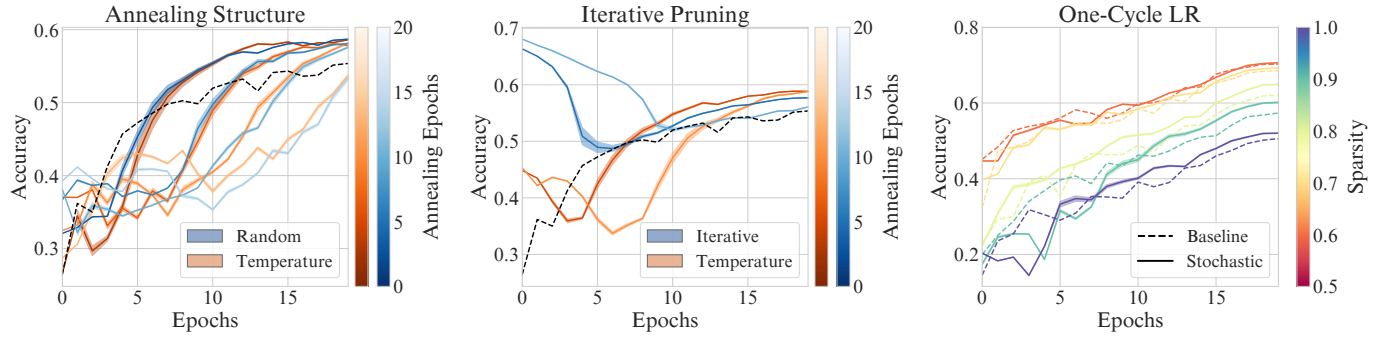


Fig. 2. Ablations over the number of annealing epochs for random annealing vs temperature annealing and temperature annealing vs iterative pruning. The rightmost graph displays the best performing annealing configuration for each sparsity and plots it against the baseline. Stochastic annealing outperformed the other methods for each sparsity when used with a one-cycle policy.

Table II. Comparison between one-shot and temperature annealing with Vision Transformers on Tiny Imagenet. We report the best accuracy for each method at various levels of target sparsity when tuned with both SGD and Adam using a constant learning rate and a one-cycle learning rate schedule. Temperature annealing consistently outperforms one-shot pruning methods for various levels of sparsity.

ViT/Tiny-ImageNet	Method	50%	60%	70%	80%	90%
SGD (Constant)	One-Shot Baseline	$38.6 \pm 0.25$	$37.8 \pm 0.31$	$29.3 \pm 0.38$	$7.1 \pm 0.68$	$3.0 \pm 0.01$
	Temperature Annealing	$40.6 \pm 0.48$	$38.3 \pm 0.19$	$30.7 \pm 0.26$	$7.1 \pm 0.24$	$3.2 \pm 0.09$
SGD (One-Cycle)	One-Shot Baseline	$42.5 \pm 0.11$	$39.6 \pm 0.21$	$33.4 \pm 0.05$	$11.4 \pm 1.46$	$5.1 \pm 0.04$
	Temperature Annealing	$42.8 \pm 0.10$	$39.8 \pm 0.08$	$33.9 \pm 0.31$	$11.7 \pm 0.61$	$6.4 \pm 0.13$
Adam (Constant)	One-Shot Baseline	$42.0 \pm 0.06$	$42.4 \pm 0.08$	$42.3 \pm 0.05$	$40.0 \pm 0.23$	$35.6 \pm 0.25$
	Temperature Annealing	$42.6 \pm 0.20$	$43.1 \pm 0.13$	$42.3 \pm 0.27$	$40.6 \pm 0.12$	$36.4 \pm 0.16$
Adam (One-Cycle)	One-Shot Baseline	$47.0 \pm 0.05$	$46.8 \pm 0.03$	$45.7 \pm 0.18$	$41.9 \pm 0.02$	$36.9 \pm 0.21$
	Temperature Annealing	$47.6 \pm 0.20$	$47.3 \pm 0.20$	$46.4 \pm 0.12$	$42.0 \pm 0.10$	$37.6 \pm 0.19$

Table II reports the mean results for each technique over three runs where we observe small yet consistent improvement with temperature annealing over one-shot pruning. This holds for both SGD and Adam with both constant and one-cycle learning rate schedules. There is a stark difference between SGD and Adam as the target networks become more sparse as Vision Transformers appear to be much more sensitive to pruning over convolutional networks.

## V. STOCHASTIC PRUNE AND TUNE ENSEMBLES

Ensemble learning is a powerful technique for improving the generalization of machine learning systems [11], [19]. These algorithms train multiple models which are then evaluated independently on test data. The combination of several predictions allows for bias and variance reduction that results in reliable performance improvement. However, as datasets and neural networks have grown larger, traditional ensemble methods have become prohibitively expensive to implement. Recent research has shown that low-cost ensemble methods can achieve performance that rivals full size ensembles at a significantly reduced cost. Several of the most powerful low-cost methods do this by leveraging sparse subnetworks within large parent networks. [12], [25], [38], [42].

Prune and Tune Ensembling (PAT) is one such technique that demonstrates excellent efficiency for the training compute/accuracy tradeoff. These work by first training a sin-

gle parent network for the majority of the training budget. Child networks are then spawned by cloning and dramatically pruning the parent using random or anti-random sampling strategies. Each of the child networks are then fine tuned with a cyclic learning rate schedule for a small number of epochs.

As child networks are all derived from an identical parent network, anti-random pruning and one-cycle tuning are used to encourage diversity and reduce correlation among ensemble members by ensuring that topological structures are distant and that parameters move far apart in optimization space before converging [31], [36], [42], [43].

Anti-random pruning creates mirrored pairs of child networks, such that whenever we randomly prune the parent to create a child, a sibling is created that inherits the opposite set of parameters. Consider a binary bit string  $M = \{x_0, \dots, x_n : x \in \{0, 1\}\}$ , that is randomly generated where 1 represents parameters that are kept and 0 represents parameters that are pruned. The anti-random network is created by reversing the polarity of all the bits in the mask  $M$ , such that:

$$\hat{\theta}_1 = \theta \circ M \quad (5)$$

$$\hat{\theta}_2 = \theta \circ (1 - M) \quad (6)$$

where  $\hat{\theta}_i$  are the parameters of the child network,  $\theta$  are the parameters of the parent network and  $\circ$  denotes the Hadamard product.

---

**Algorithm 1:** Stochastic Prune and Tune Ensembles

---

**Input:**  $N$ , the number of ensemble members  
**Input:**  $(X_{train}, X_{test})$ , the training and test data  
**Input:**  $(t_{parent}, t_{child}, t_{anneal})$ , the number of parent, child, and annealing epochs  
**Input:**  $(\eta_{parent}, \eta_{child})$ , the parent and child optimizer hyperparameters  
**Input:**  $\phi(\rho)$ , the subnetwork sampling process with target sparsity  $\rho$   
**Input:**  $\Theta(M, \tau, e, t)$ , the temperature scaling function applied to a mask  $M$ , with initial temperature  $\tau$ , for current epoch  $e$ , over  $t$  total annealing epochs

```

 $O = \text{optimizer}(\eta_{parent})$ 
 $F = \text{initialize}()$ 
 $F.w = \text{train}(F, O, X_{train}, t_{parent})$ 

ensemble = []

for  $i$  in  $1$  to  $N$  do
   $f_i = \text{initialize}()$ 
   $f_i.w = F.w$ 

  for  $j$  in  $f_i.layers$  do
     $| M_j \sim \phi(\rho)^{f_i.j.w}$ 
  end

   $O = \text{optimizer}(\eta_{child})$ 

  for  $e$  in  $t_{child}$  do
     $P \leftarrow \Theta(M, \tau, e, t_{anneal})$ 

    for  $(x, y)$  in  $X_{train}$  do
       $| \hat{f}_i.w \leftarrow f_i.w \circ \text{Bernoulli}(P)$ 
       $| f_i.w = \text{train}(\hat{f}_i, O, (x, y))$ 
    end
  end

   $ensemble \leftarrow f_i$ 
end

for  $(x, y)$  in  $X_{test}$  do
   $| outputs = [F(x), c(x) \text{ for } c \text{ in ensemble}]$ 
   $| predictions = \text{softmax}(\text{mean}(outputs))$ 
end

```

---

Stochastic Subnetwork Annealing can be naturally implemented to tune child networks within the context of this low-cost ensemble algorithm. Random annealing also extends to the ideas of anti-random pruning through anti-probability matrices. When a probability matrix is generated, a mirrored probability matrix can be generated such that the subnetworks anneal to opposite topological structures  $P' = 1 - P$ .

We evaluate the efficacy of Stochastic Subnetwork Annealing in this context via a benchmark low-cost ensemble comparison on CIFAR-10 and CIFAR-100 with WideResnet-28x10. We include results for these ensembles on corrupted versions of the CIFAR datasets as well, in order to test robustness on out-of-distribution images [33]. These corrupted datasets are generated by adding 20 different kinds of image corruptions (gaussian noise, snow, blur, pixelation, etc.) at five different levels of severity to the original test sets. The total number of images in each of these additional sets is 1,000,000.

We take the training configuration, ensemble size and parameter settings directly from studies of three state-of-the-art benchmark low-cost ensemble methods: MotherNets [39], Snapshot Ensembles [15], and Fast Geometric Ensembles [7]. We also compare our results with published results of several recent low-cost ensemble methods including: TreeNets [22], BatchEnsemble [41], FreeTickets [25], and MIMO [12].

All methods compared use the same WideResnet model and are optimized using Stochastic Gradient Descent with Nesterov momentum  $\mu = 0.9$  and weight decay  $\gamma = 0.0005$ . The ensemble size and training schedule is as used in previous comparisons [7], [39]. We use a batch size of 128 for training and use random crop, random horizontal flip, and mean standard normalization data augmentations for all approaches [7], [12], [15], [26]. The parent learning rate uses a step-wise decay schedule. An initial learning rate of  $\eta_1 = 0.1$  is used for 50% of the training budget which decays linearly to  $\eta_2 = 0.001$  at 90% of the training budget. The learning rate is kept constant at  $\eta_2 = 0.001$  for the final 10% of training.

We train a single parent network for 140 epochs. Six children are then created by randomly pruning 50% of the connections in the parent network. Neural partitioning is implemented where pairs of children are generated with opposite sets of inherited parameters. Each child is tuned with a one-cycle learning rate for 10 epochs. The tuning schedule starts at  $\eta_1 = 0.001$ , increases to  $\eta_2 = 0.1$  at 1 epoch and then decays to  $\eta_3 = 1e-7$  using cosine annealing for the final 9 epochs.

We implement Stochastic Annealing when tuning the child networks by using the procedure illustrated above for Temperature Annealing. We initialize the binary subnetwork masks with a target sparsity of 0.5. We then modify the masks such that the 0 parameters are initialized with a temperature of  $\tau = 0.5$ . That value is decayed to  $\tau = 0$  over 3 annealing epochs using a cosine decay.

The Independent Model is a single WideResNet-28-10 model trained for 200 Epochs. The Dropout Model includes dropout layers between convolutional layers in the residual blocks at a rate of 30% [45]. Snapshot Ensembles use a cosine annealing learning rate with an initial learning rate  $\eta = 0.1$  for a cycle length of 40 epochs [15]. Fast Geometric Ensembles use a pre-training routine for 156 epochs. A curve finding algorithm then runs for 22 epochs with a cycle length of 4, each starting from checkpoints at epoch 120 and 156. TreeNets, [22], BatchEnsemble [41] and Multiple-Input Multiple-Output [12] are all trained for 250 epochs. FreeTickets introduces several configurations for building ensembles. We include their

Table III. Results for ensembles of WideResNet-28-10 models on both CIFAR-10 and CIFAR-100. Methods with \* denote results obtained from [12], [26]. Best low-cost ensemble results are **bold**. cAcc, cNLL, and cECE correspond to corrupted test sets. M corresponds to the number of models in the ensemble. We report the mean values over 10 runs for Prune and Tune and Temperature Annealing.

Methods (CIFAR-10/WRN-28-10)	Acc $\uparrow$	NLL $\downarrow$	ECE $\downarrow$	cAcc $\uparrow$	cNLL $\downarrow$	cECE $\downarrow$	Epochs $\downarrow$
Independent Model*	96.0	0.159	0.023	76.1	1.050	0.153	200
Monte Carlo Dropout*	95.9	0.160	0.024	68.8	1.270	0.166	200
Snapshot (M=5)	96.3	0.131	0.015	76.0	1.060	0.121	200
Fast Geometric (M=12)	96.3	0.126	0.015	75.4	1.157	0.122	200
Prune and Tune (M=6)	96.5	0.113	0.005	76.2	0.972	0.081	200
Temperature Annealing (M=6, $\tau=0.5$ , e=3)	<b>96.7</b>	<b>0.110</b>	<b>0.005</b>	<b>76.3</b>	<b>0.968</b>	<b>0.079</b>	<b>200</b>
TreeNet (M=3)*	95.9	0.258	0.018	75.5	0.969	0.137	250
BatchEnsemble (M=4)*	96.2	0.143	0.021	77.5	1.020	0.129	250
Multi-Input Multi-Output (M=3)*	96.4	0.123	0.010	76.6	0.927	0.112	250
FreeTickets (EDST) (M=7)*	96.4	0.127	0.012	76.7	0.880	0.100	850
FreeTickets (DST) (M=3)*	96.4	0.124	0.011	77.6	0.840	0.090	750
Dense Ensemble (M=4)*	96.6	0.114	0.010	77.9	0.810	0.087	800

Methods (CIFAR-100/WRN-28-10)	Acc $\uparrow$	NLL $\downarrow$	ECE $\downarrow$	cAcc $\uparrow$	cNLL $\downarrow$	cECE $\downarrow$	Epochs $\downarrow$
Independent Model*	79.8	0.875	0.086	51.4	2.700	0.239	200
Monte Carlo Dropout*	79.6	0.830	0.050	42.6	2.900	0.202	200
Snapshot (M=5)	82.1	0.661	0.040	52.2	2.595	0.145	200
Fast Geometric (M=12)	82.3	0.653	0.038	51.7	2.638	0.137	200
Prune and Tune (M=6)	82.7	0.634	0.013	52.7	2.487	0.131	200
Temperature Annealing (M=6, $\tau=0.5$ , e=3)	<b>83.1</b>	<b>0.633</b>	<b>0.010</b>	<b>52.8</b>	<b>2.440</b>	<b>0.131</b>	<b>200</b>
TreeNet (M=3)*	80.8	0.777	0.047	53.5	2.295	0.176	250
BatchEnsemble (M=4)*	81.5	0.740	0.056	54.1	2.490	0.191	250
Multi-Input Multi-Output (M=3)*	82.0	0.690	0.022	53.7	2.284	0.129	250
FreeTickets (EDST) (M=7)*	82.6	0.653	0.036	52.7	2.410	0.170	850
FreeTickets (DST) (M=3)*	82.8	0.633	0.026	54.3	2.280	0.140	750
Dense Ensemble (M=4)*	82.7	0.666	0.021	54.1	2.270	0.138	800

two best configurations for Dynamic Sparse Training (DST, M=3, S=0.8) and Efficient Dynamic Sparse Training (EDST, M=7, S=0.9).

We compare the results of our approach to a wide variety of competitive benchmarks which include both low-cost and full-size ensemble approaches. The details for these implementations are taken from baseline results reported in [12], [25], [42], and is informed by each original implementation in [7], [12], [15], [22], [41]. We observe improved performance with temperature annealing over these established methods on both CIFAR-10 and CIFAR-100.

## VI. CONCLUSIONS

Stochastic Subnetwork Annealing offers a novel approach to tuning pruned models by representing subnetworks with probabilistic masks. Rather than discretely removing parameters, we instead create probability matrices that alter the chance for parameters to be retained on any given forward pass. The probability values are then annealed towards a deterministic binary mask over several epochs such that the subnetwork is slowly revealed. We introduce several variations of Subnetwork Annealing, including Random Annealing, which uses random probabilities for every parameter, and Temperature Annealing, which applies an even amount of stochasticity governed by a hyperparameter value  $\tau$ .

The efficacy of Stochastic Subnetwork Annealing is built upon the principles behind iterative pruning. Instead of pruning a large number of parameters at once, which can lead to a destructive effect on convergence quality, Stochastic Annealing slowly evolves subnetworks over time. Recent insights in optimization research have revealed that early epochs are critical during optimization as they set the foundational trajectory for the rest of the training process. [8], [9], [30]. Stochastic Subnetwork Annealing provides effective regularization during the early epochs of subnetwork tuning to promote training stability and encourage robust adaptation.

Stochastic Subnetwork Annealing is flexible with a variety of hyperparameter choices to fit a wide range of learning tasks, network architectures, and optimization goals. Annealing towards a deterministic binary structure allows for probability matrices to be tossed out after tuning, resulting in small and sparse networks that are able to take advantage of hardware optimization during inference. Our extensive ablation studies explore the dynamics of Stochastic Annealing with regard to different network architectures, benchmark datasets, annealing configurations, pruning methodologies, and optimization hyperparameters.

We observe marked improvement over established one-shot and iterative pruning benchmarks in a wide variety of cases. This technique is especially effective for ResNets at high levels

of sparsity (95-98%), and we see a similar performance gain with Vision Transformers on the more difficult Tiny Imagenet dataset. We additionally demonstrate the utility of this method in the context of a low-cost ensemble learning algorithm called Prune and Tune Ensembles, where we used Stochastic Annealing to fine tune the child networks to achieve increased generalization and robustness performance over benchmark methods, resulting in better accuracy than methods that require 4-5x more training compute. Stochastic Annealing is an elegant and flexible technique that can be used to better tune sparse subnetworks obtained from trained parent models.

## REFERENCES

- [1] Davis Blalock, Jose Javier Gonzalez Ortiz, Jonathan Frankle, and John Guttag. What is the state of neural network pruning?, 2020.
- [2] Ekin D. Cubuk, Barret Zoph, Dandelion Mane, Vijay Vasudevan, and Quoc V. Le. Autoaugment: Learning augmentation policies from data, 2019.
- [3] Alexey Dosovitskiy, Lucas Beyer, Alexander Kolesnikov, Dirk Weissenborn, Xiaohua Zhai, Thomas Unterthiner, Mostafa Dehghani, Matthias Minderer, Georg Heigold, Sylvain Gelly, Jakob Uszkoreit, and Neil Houlsby. An image is worth 16x16 words: Transformers for image recognition at scale, 2021.
- [4] Sara Elkerdawy, Mostafa Elhoushi, Hong Zhang, and Nilanjan Ray. Fire together wire together: A dynamic pruning approach with self-supervised mask prediction, 2022.
- [5] Jonathan Frankle and Michael Carbin. The lottery ticket hypothesis: Finding sparse, trainable neural networks, 2019.
- [6] Trevor Gale, Erich Elsen, and Sara Hooker. The state of sparsity in deep neural networks, 2019.
- [7] Timur Garipov, Pavel Izmailov, Dmitrii Podoprikin, Dmitry Vetrov, and Andrew Gordon Wilson. Loss surfaces, mode connectivity, and fast ensembling of dnns, 2018.
- [8] Justin Gilmer, Behrooz Ghorbani, Ankush Garg, Sneha Kudugunta, Behnam Neyshabur, David Cardoze, George Dahl, Zachary Nado, and Orhan Firat. A loss curvature perspective on training instability in deep learning, 2021.
- [9] Akhilesh Gotmare, Nitish Shirish Keskar, Caiming Xiong, and Richard Socher. A closer look at deep learning heuristics: Learning rate restarts, warmup and distillation, 2018.
- [10] Song Han, Jeff Pool, John Tran, and William J. Dally. Learning both weights and connections for efficient neural networks, 2015.
- [11] L.K. Hansen and P. Salamon. Neural network ensembles. *IEEE Transactions on Pattern Analysis and Machine Intelligence*, 12(10):993–1001, 1990.
- [12] Marton Havasi, Rodolphe Jenatton, Stanislav Fort, Jeremiah Zhe Liu, Jasper Snoek, Balaji Lakshminarayanan, Andrew M. Dai, and Dustin Tran. Training independent subnetworks for robust prediction, 2021.
- [13] Kaiming He, Xiangyu Zhang, Shaoqing Ren, and Jian Sun. Deep residual learning for image recognition. In *IEEE Computer Vision and Pattern Recognition (CVPR)*, pages 770–778, 2016.
- [14] Weizhe Hua, Yuan Zhou, Christopher De Sa, Zhiru Zhang, and G. Edward Suh. Channel gating neural networks, 2019.
- [15] Gao Huang, Yixuan Li, Geoff Pleiss, Zhuang Liu, John E. Hopcroft, and Kilian Q. Weinberger. Snapshot ensembles: Train 1, get m for free, 2017.
- [16] Diederik P. Kingma and Jimmy Ba. Adam: A method for stochastic optimization, 2017.
- [17] Diederik P. Kingma, Tim Salimans, and Max Welling. Variational dropout and the local reparameterization trick, 2015.
- [18] Alex Krizhevsky. Learning multiple layers of features from tiny images. *Technical Report, University of Toronto*, May 2012.
- [19] Anders Krogh and Jesper Vedelsby. Neural network ensembles, cross validation, and active learning. In G. Tesauro, D. Touretzky, and T. Leen, editors, *Advances in Neural Information Processing Systems*, volume 7. MIT Press, 1994.
- [20] Ya Le and Xuan S. Yang. Tiny imagenet visual recognition challenge, 2015.
- [21] Jaeho Lee, Sejun Park, Sangwoo Mo, Sungsoo Ahn, and Jinwoo Shin. Layer-adaptive sparsity for the magnitude-based pruning, 2021.
- [22] Stefan Lee, Senthil Purushwalkam, Michael Cogswell, David Crandall, and Dhruv Batra. Why m heads are better than one: Training a diverse ensemble of deep networks. *arXiv preprint:1511.06314*, 2015.
- [23] Hao Li, Asim Kadav, Igor Durdanovic, Hanan Samet, and Hans Peter Graf. Pruning filters for efficient convnets, 2017.
- [24] Ji Lin, Yongming Rao, Jiwen Lu, and Jie Zhou. Runtime neural pruning. In I. Guyon, U. Von Luxburg, S. Bengio, H. Wallach, R. Fergus, S. Vishwanathan, and R. Garnett, editors, *Advances in Neural Information Processing Systems*, volume 30. Curran Associates, Inc., 2017.
- [25] Shiwei Liu, Tianlong Chen, Zahra Atashgahi, Xiaohan Chen, Ghada Sokar, Elena Mocanu, Mykola Pechenizkiy, Zhangyang Wang, and Decebal Constantin Mocanu. Deep ensembling with no overhead for either training or testing: The all-round blessings of dynamic sparsity, 2022.
- [26] Shiwei Liu, Tianlong Chen, Zahra Atashgahi, Xiaohan Chen, Ghada Sokar, Elena Mocanu, Mykola Pechenizkiy, Zhangyang Wang, and Decebal Constantin Mocanu. Deep ensembling with no overhead for either training or testing: The all-round blessings of dynamic sparsity, 2022.
- [27] Shiwei Liu, Tianlong Chen, Xiaohan Chen, Li Shen, Decebal Constantin Mocanu, Zhangyang Wang, and Mykola Pechenizkiy. The unreasonable effectiveness of random pruning: Return of the most naive baseline for sparse training, 2022.
- [28] Zhuang Liu, Mingjie Sun, Tinghui Zhou, Gao Huang, and Trevor Darrell. Rethinking the value of network pruning, 2019.
- [29] Jerry Ma and Denis Yarats. On the adequacy of untuned warmup for adaptive optimization, 2019.
- [30] Jerry Ma and Denis Yarats. On the adequacy of untuned warmup for adaptive optimization, 2021.
- [31] Yashwant Malaiya. Antirandom testing: getting the most out of black-box testing. In *Proceedings of Sixth International Symposium on Software Reliability Engineering. ISSRE’95*, pages 86 – 95, 1995.
- [32] Dmitry Molchanov, Arsenii Ashukha, and Dmitry Vetrov. Variational dropout sparsifies deep neural networks, 2017.
- [33] Zachary Nado, Neil Band, Mark Collier, Josip Djolonga, Michael Dusenberry, Sebastian Farquhar, Angelos Filos, Marton Havasi, Rodolphe Jenatton, Ghassen Jerfel, Jeremiah Liu, Zelda Mariet, Jeremy Nixon, Shreyas Padhy, Jie Ren, Tim Rudner, Yeming Wen, Florian Wenzel, Kevin Murphy, D. Sculley, Balaji Lakshminarayanan, Jasper Snoek, Yarin Gal, and Dustin Tran. Uncertainty Baselines: Benchmarks for uncertainty & robustness in deep learning. *arXiv preprint arXiv:2106.04015*, 2021.
- [34] Omita. Vit-cifar. <https://github.com/omihub777/ViT-CIFAR>, 2022.
- [35] Alex Renda, Jonathan Frankle, and Michael Carbin. Comparing rewinding and fine-tuning in neural network pruning, 2020.
- [36] Leslie N. Smith and Nicholay Topin. Super-convergence: Very fast training of neural networks using large learning rates, 2018.
- [37] Nitish Srivastava, Geoffrey Hinton, Alex Krizhevsky, Ilya Sutskever, and Ruslan Salakhutdinov. Dropout: A simple way to prevent neural networks from overfitting. *Journal of Machine Learning Research*, 15(56):1929–1958, 2014.
- [38] Johannes von Oswald, Seiji Kobayashi, Alexander Meulemans, Christian Henning, Benjamin F. Grewe, and João Sacramento. Neural networks with late-phase weights, 2022.
- [39] Abdul Wasay, Brian Hentschel, Yuze Liao, Sanyuan Chen, and Stratos Idreos. Mothnets: Rapid deep ensemble learning. *arXiv preprint:1809.04270*, 2018.
- [40] Wei Wen, Chunpeng Wu, Yandan Wang, Yiran Chen, and Hai Li. Learning structured sparsity in deep neural networks, 2016.
- [41] Yeming Wen, Dustin Tran, and Jimmy Ba. Batchensemble: An alternative approach to efficient ensemble and lifelong learning, 2020.
- [42] Tim Whitaker and Darrell Whitley. Prune and tune ensembles: Low-cost ensemble learning with sparse independent subnetworks, 2022.
- [43] Shen Wu, Jandhyala Sridhar, Yashwant Malaiya, and Anura Jayasumana. Antirandom testing: A distance-based approach. *Journal of VLSI Design*, 2008.
- [44] Kaichao You, Mingsheng Long, Jianmin Wang, and Michael I. Jordan. How does learning rate decay help modern neural networks?, 2019.
- [45] Sergey Zagoruyko and Nikos Komodakis. Wide residual networks, 2017.
- [46] Xiaohua Zhai, Alexander Kolesnikov, Neil Houlsby, and Lucas Beyer. Scaling vision transformers, 2022.